

Electronic Supporting Information (ESI) for:
**Novel Colour-based, Prototype Indicator for use in High
Pressure Processing (HPP)**

Dilidaer Yusufu, Michael Bingham and Andrew Mills*

School of Chemistry and Chemical Engineering, Queens University Belfast, David Keir
Building, Stranmillis Road, Belfast, BT95AG, UK

S1: Examples of typical HPP conditions used to process different foods

Table S1: Examples of the different HPP conditions used to treat various foodstuffs.

Food group	Time (min)	Temperature °C	Pressure (MPa)	Ref
Tomato juice	1	75	600	[1]
Apple and orange juice	1-3	20	500	[2]
Soy Smoothies	3	20	450-650	[3]
Aloe Vera Gel	3	20	400	[4]
Kiwi puree	3	20-25	500	[5]
Strawberry Juice	3	38	600	[6]
Milk	3	30	600	[7]

S2: Water-impermeable clear plastic polymer film

The water-impermeable clear plastic polymer film used to encapsulate the indicator components was provided by Sensor Indicator Products, and the cross-section schematic of the polymer film was given below:

12.5 μm PET + ALO coating
19 μm LDPE
12.5 μm PET + ALO coating
19 μm LDPE
50 μm Coex film (peelable)

Figure S1: Cross section schematic of the water-impermeable clear plastic polymer film

S3: Pressure vs time profile of the Quintus Food Press HPP reactor, QFP 35 L-600

A typical pressure versus time, and vessel temperature versus time profile used to test the HPP indicators is illustrated in Figure S2 below:

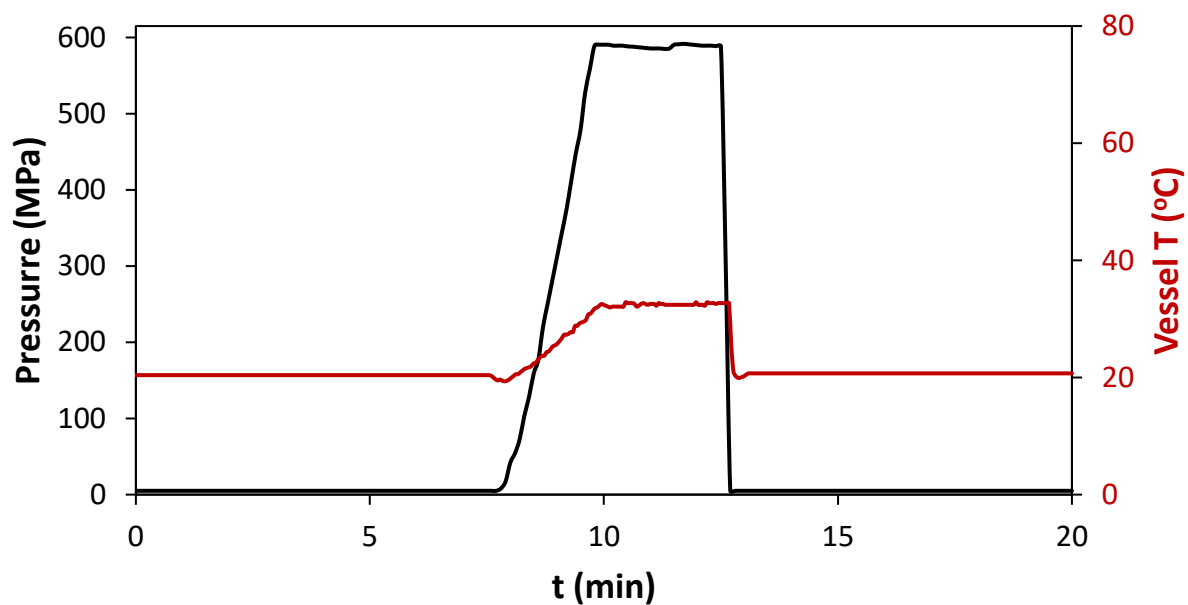


Figure S2: A typical pressure vs time, and vessel temperature vs time profile of HPP reactor when pressure is set at 600 MPa and hold time is 3 min, where before pressurisation the vessel temperature is 21°C, and 32°C when it reached 600 MPa.

S4: Congo red (CR)

Congo red is a well-known azo dye which changes colour at low pH due to protonation of its amino groups and results shifts of electrons in the aromatic ring and azo-bonds [8]. The position of amino group favours the formation of a relatively stable resonance form of ortho-chinoid derivative [9]. The protonation of CR amino groups takes place at pH 4.5–5.5 and is associated with spectral transition. The positive charge, which appears as the result of protonation of the amino groups, balances the charge of sulphonic groups and decreases the repulsion between molecules. The deprotonated (red) form and protonated (blue) form of the CR dye are shown in Figure S3.

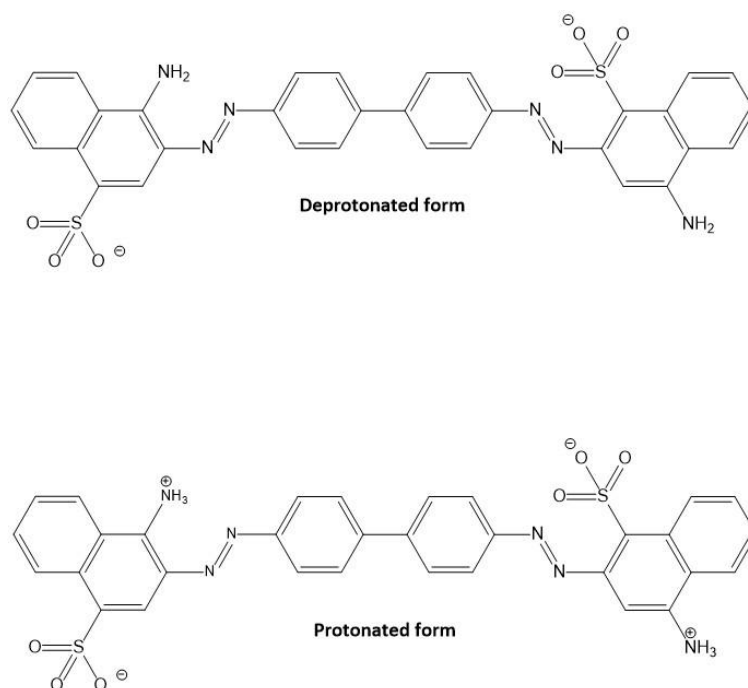


Figure S3: Structures of the deprotonated (red) and protonated (blue) congo red.

S5: Interference analysis of the CR ink film

The interference method for measuring the thickness of non-tapered, uniform thin films was proposed by Swanepoel [10], who predicted that, such film would exhibit a spectrum that had a series of interference maxima and minima, as illustrated in Figure S4, with integer, α , values 0, 1, 2, etc, starting from the longest wavelength peak, or trough.

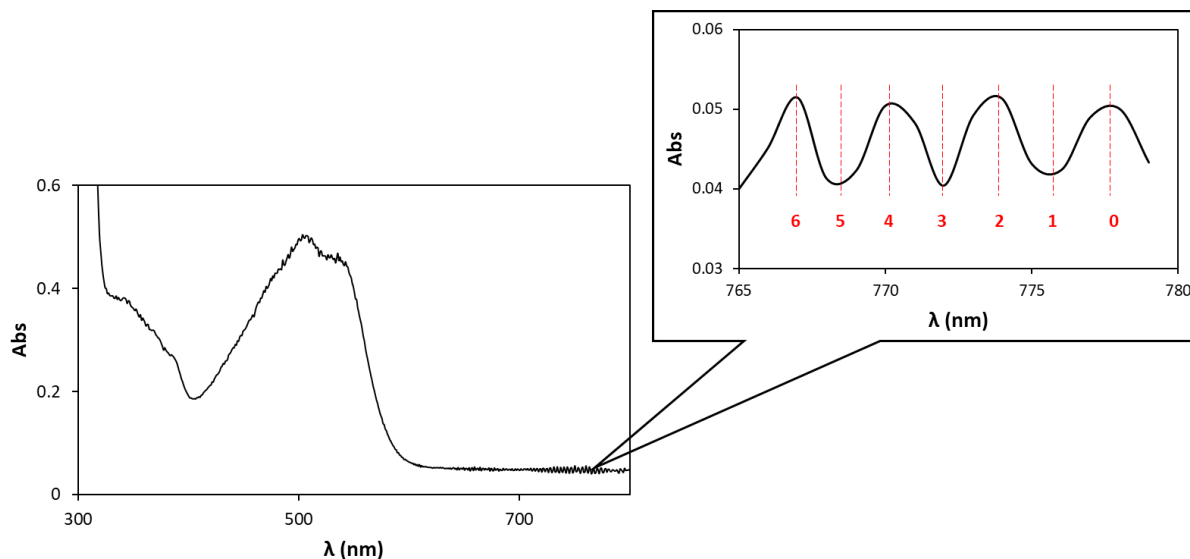


Figure S4: UV/vis absorption spectra of the CR ink film in ambient air and interference bands, $\alpha = 0$ to 6 are numbered and highlighted by the broken red lines.

Swanepoel showed that, in such a system, α is related to the thickness of the film, b , via the expression [10]:

$$\alpha/2 = 2b(n_f/\lambda) - m_o$$

where n_f is the refractive index of the film, λ is the wavelength of the peak or trough associated with the value of α and m_o is the order number of the first extreme. For example, from the data in Figure S4, seven α and λ pairs, were gleaned and then used to generate the subsequent straight-line plot, illustrated in Figure S5, of $\alpha/2$ vs n_f/λ , where n_f was taken to be that of PVA, i.e. 1.575. [11] From the gradient of this plot a value of 54.8 μm was obtained for b .

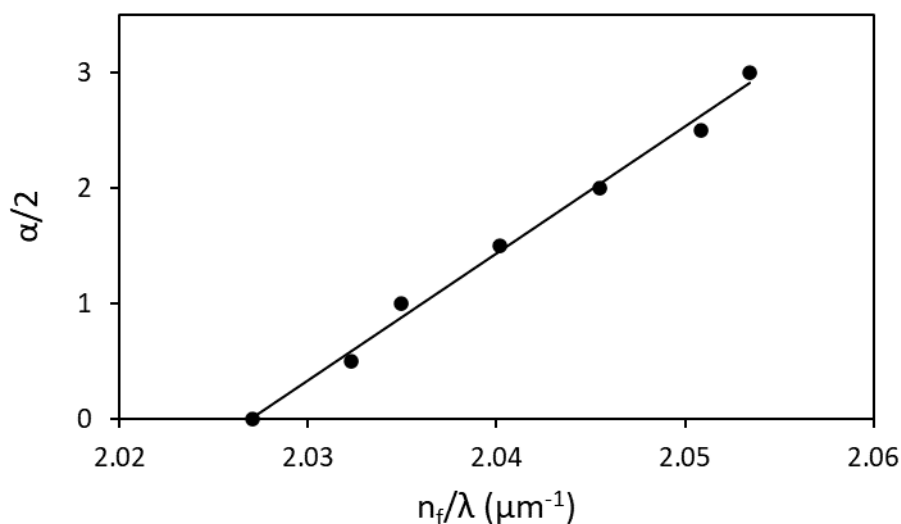


Figure S5: Plot of interference data from Figure S4 in the form of $\alpha/2$ vs n_f/λ . The gradient ($= 2b$) of the line of best fit is $109.5 \mu\text{m}$, thus, $b = 54.8 \mu\text{m}$ for the CR ink film.

Since the thickness calculated above is the thickness of CR ink film with clear PET film that CR ink film coated on, same method was used to calculated the thickness of clear PET film.

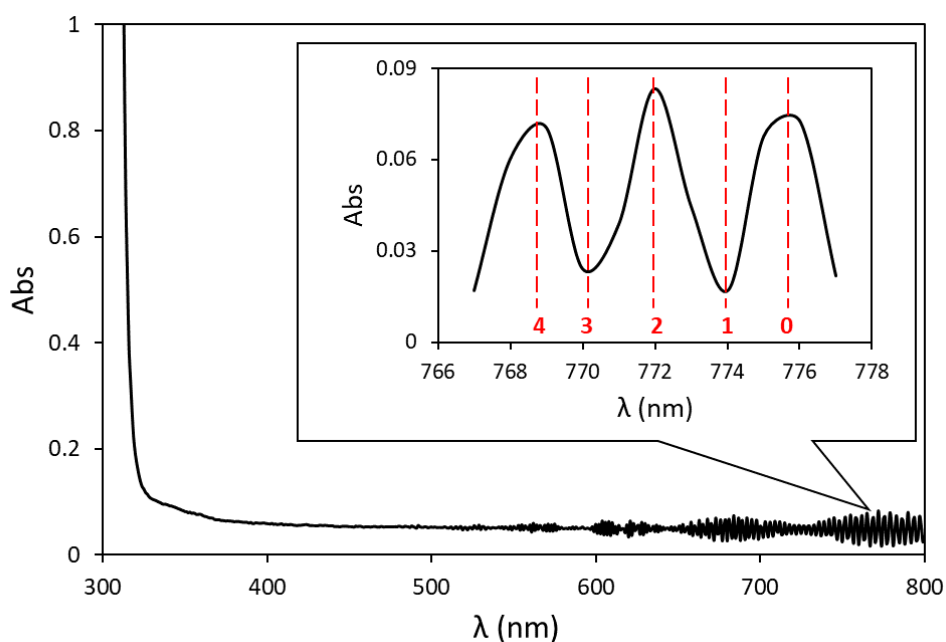


Figure S6: UV/vis absorption spectra of the clear PET film and interference bands, $\alpha = 0$ to 4 are numbered and highlighted by the broken red lines.

Using the data points shown in Figure S6, $\alpha/2$ vs n_f/λ plot is shown in Figure S7 where $n_f = 1.575$ and the calculated thickness of the clear PET film $b = 51.8 \mu\text{m}$. Hence the thickness of the CR ink film alone is $3 \mu\text{m}$.

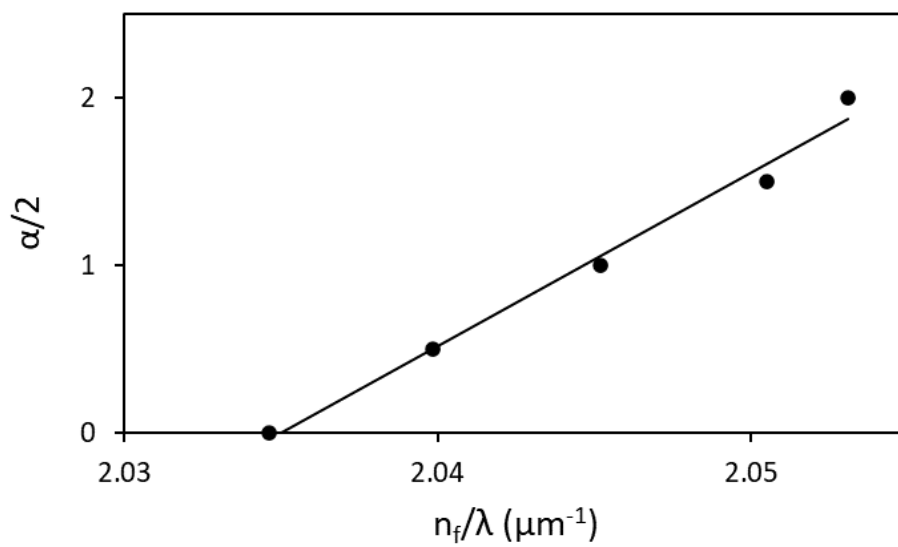


Figure S7: Plot of interference data from Figure S6 in the form of $\alpha/2$ vs n_f/λ . The gradient ($= 2b$) of the line of best fit is $103.6 \mu\text{m}$, thus, $b = 51.8 \mu\text{m}$ for the clear PET film.

References

1. Daryaei, H.; Balasubramaniam, V. Kinetics of *Bacillus coagulans* spore inactivation in tomato juice by combined pressure–heat treatment. *Food Control* **2013**, *30*, 168-175.
2. Shahbaz, H.M.; Yoo, S.; Seo, B.; Ghafoor, K.; Kim, J.U.; Lee, D.-U.; Park, J. Combination of TiO₂-UV photocatalysis and high hydrostatic pressure to inactivate bacterial pathogens and yeast in commercial apple juice. *Food and bioprocess technology* **2016**, *9*, 182-190.
3. Andrés, V.; Villanueva, M.-J.; Tenorio, M.-D. Influence of high pressure processing on microbial shelf life, sensory profile, soluble sugars, organic acids, and mineral content of milk-and soy-smoothies. *LWT-food Science and Technology* **2016**, *65*, 98-105.
4. Reyes, J.E.; Guanoquiza, M.I.; Tabilo-Munizaga, G.; Vega-Galvez, A.; Miranda, M.; Pérez-Won, M. Microbiological stabilization of Aloe vera (*Aloe barbadensis* Miller) gel by high hydrostatic pressure treatment. *International journal of food microbiology* **2012**, *158*, 218-224.
5. Fernández-Sestelo, A.; de Saá, R.S.; Pérez-Lamela, C.; Torrado-Agrasar, A.; Rúa, M.L.; Pastrana-Castro, L. Overall quality properties in pressurized kiwi purée: microbial, physicochemical, nutritive and sensory tests during refrigerated storage. *Innovative Food Science & Emerging Technologies* **2013**, *20*, 64-72.
6. Pan, H.; Buenconsejo, M.; Reineke, K.F.; Shieh, Y.C. Effect of process temperature on virus inactivation during high hydrostatic pressure processing of contaminated fruit puree and juice. *Journal of food protection* **2016**, *79*, 1517-1526.
7. Stratakis, A.C.; Inguglia, E.S.; Linton, M.; Tollerton, J.; Murphy, L.; Corcionivoschi, N.; Koidis, A.; Tiwari, B.K. Effect of high pressure processing on the safety, shelf life and quality of raw milk. *Innovative Food Science & Emerging Technologies* **2019**, *52*, 325-333.
8. Panczyk, T.; Wolski, P.; Jagusiak, A.; Drach, M. Molecular dynamics study of Congo red interaction with carbon nanotubes. *RSC Advances* **2014**, *4*, 47304-47312.
9. Spólnik, P.; Stopa, B.; Piekarska, B.; Jagusiak, A.; Konieczny, L.; Rybarska, J.; Król, M.; Roterman, I.; Urbanowicz, B.; Zięba-Palus, J. The Use of Rigid, Fibrillar Congo Red Nanostructures for Scaffolding Protein Assemblies and Inducing the Formation of Amyloid-like Arrangement of Molecules. *Chemical biology & drug design* **2007**, *70*, 491-501.
10. Swanepoel, R. Determination of the thickness and optical constants of amorphous silicon. *Journal of Physics E: Scientific Instruments* **1983**, *16*, 1214.
11. Polymer Properties Database. Available online: <http://polymerdatabase.com/polymer%20physics/Ref%20Index%20Table%20.html> (accessed on May 2021).